

MECHANICAL EVALUATION OF ADDITIVELY MANUFACTURED COMPOSITE MATERIALS FABRICATED USING MARKFORGED X7

Barroeta Robles, Julieta^{1*}, Wanjara, Priti¹, Cole, Richard. G¹, Sanchez, Fabian², Spineanu, Andrew², Chkafi, Anas², Gholipour, Javad¹

¹ National Research Council Canada, Aerospace Manufacturing Technologies Centre, Montreal and Ottawa, Canada

² Siemens Canada Ltd. (In collaboration with the government of Quebec), Montreal, Canada

* Corresponding author (Julieta.BarroetaRobles@cnrc-nrc.gc.ca)

Keywords: *Additive manufacturing, tensile testing, fatigue testing*

ABSTRACT

Advanced composite materials have been used in the aerospace industry due to their advantageous properties, such as high strength-to-weight ratios, high toughness and fatigue resistance. There are different manufacturing processes and techniques that have been used to produce composite parts. Over the last few years, the increasing interest in thermoplastic materials has allowed the growth of processes, such as additive manufacturing (AM), to produce components used in the automotive and aerospace industry. This process facilitates the fabrication of complex parts with high tolerances from a three-dimensional (3D) model. For instance, the fused filament fabrication (FFF) process is an AM technology that uses a continuous filament of thermoplastic material. This filament gets deposited on the surface of a build plate and the part is created by building up layers.

In this work, the potential of AM for next generation engine applications was explored using FFF technology in a Markforged X7 3D industrial printer to manufacture continuous carbon fibre reinforced specimens with an Onyx™ matrix (i.e., nylon with chopped carbon fibre). Specimens were printed as a length-oversized “racetrack” and these were machined into coupons to be tested in tension and in fatigue as per ASTM D3039 and ASTM D3479, respectively. A method was established to machine these coupons without inducing delaminations in the material. Three printing configurations were evaluated during this work: concentric (CC), quasi-isotropic (QI), and Onyx™ only (OO). These specimens were all printed with an Onyx™-only outer layer in the walls, roofs and floors (i.e., outside edges, highest and lowest layers of the specimens, respectively) that is standard on the Markforged system for finishing purposes. In quasi-static tensile testing, the OO baseline configuration exhibited an ultimate tensile strength (UTS) of 29 MPa, a modulus of 0.4 GPa and ductile failure perpendicular to the printing direction. For the QI configuration, the UTS (245 MPa) and modulus (18 GPa) were considerably improved over the OO configuration. The CC configuration resulted in the highest UTS of 707 MPa and modulus of 54 GPa, due to alignment of the fibres with the loading direction. Tensile failure of the CC and QI coupons occurred in several locations due to delamination and pull-out of some fibre strands. The QI samples were evaluated in fatigue testing and survival at 10⁶ cycles was observed for coupons tested at 25% and 50% of the UTS (245 MPa). Coupons cycled at 65% of the UTS showed significant variability in cycles to failure, without surviving the full test range. Examination of the fracture surface revealed voids and discontinuous regions that may be due to the printing process.

1 INTRODUCTION

Advanced composite materials have been used in aerospace for several years due to their high strength-to-weight ratios, thermal stabilities, and their mechanical properties. In particular, carbon fibre reinforced polymer composites (CFRP) have been fabricated using different manufacturing processes, such as hand lay-up, autoclave and out-of-autoclave processing, and compression and injection moulding. These processes allow the production of high performance parts, however, it can be difficult to fabricate components with complex and hollow structures. Additive manufacturing (AM) has been identified as an alternative to these processes to manufacture complex structures at a low cost, as it can shorten the manufacturing cycle time, while attaining high performance [1, 2].

In particular, Fused Filament Fabrication (FFF) has been identified as a promising technology. This AM technique consists of laying down thermoplastic filament, which is melted and fused together, layer-by-layer to build a part [3]. A diagram of this technique is shown in Figure 1. The filament is fed into a head and extruded as a molten bead above the glass transition temperature (T_g) or the melting temperature (T_m), for amorphous or semi-crystalline thermoplastic materials, respectively. The first layer is deposited onto the printing bed, and subsequent layers are then deposited above this first layer until the part is completed. Some systems allow for the inclusion of continuous reinforcing fibres within the extruded material, thereby allowing the direct manufacture of a CFRP part.

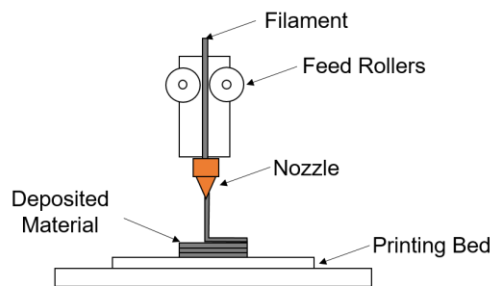


Figure 1: Diagram of a FFF setup

In this paper, a field-deployable industrial-grade three-dimensional (3D) printer, Markforged X7, was used to manufacture specimens in order to evaluate the performance of different material configurations, which included different layups, matrix and reinforcement combinations. These efforts were conducted to support sustainable engineering, design, and the production of the next-generation industrial engine components. The purpose of this research was to characterize the mechanical properties of samples printed by FFF, in particular the quasi-static tensile strength and modulus, and fatigue in tension-tension. The outcome of this work provided a deeper understanding of this technology and an evaluation of how to expand it to other applications that go beyond the current uses for tooling and prototyping.

2 EXPERIMENTAL

2.1 Materials

In this paper, the FFF Markforged X7 system was used. This 3D printer is an industrial grade platform featuring a dual nozzle print system, which is able to print polymer matrices along with a variety of continuous reinforcements, such as carbon, glass fibre, and Kevlar, with Z-layer resolutions ranging from 50 μm up to 250 μm [4]. In this work, only carbon fibre reinforcement and Onyx™ as the polymer matrix were evaluated. Onyx™ consists of a mixture of Nylon with chopped carbon fibre [5].

To characterize the mechanical performance, continuous carbon fibre specimens were printed as an oversized “racetrack”, as shown in Figure 2. The commercial 3D printing software provided by Markforged, Eiger, was used to design and print the samples with and without reinforcement (i.e., carbon fibre reinforced vs. Onyx™-only). The specimens printed for this work by the authors included a finishing feature, which could not be removed from the printed samples as it is a default setting in the Eiger software. The specimens contained single-bead wide external Onyx™-only “walls”, “roofs” (i.e., the top-most layer), and “floors” (i.e., the bottom-most layer). An additional set of samples was provided by Markforged, which did not have any such walls, roofs, or floors (labelled MF in this paper). The three configurations that were printed and explored by the authors were concentric (CC), quasi-isotropic (QI), and Onyx™-only (OO), using the bead lay-up orientations listed in Table 1.



Figure 2: “Racetrack” configuration used to 3D print samples to characterize with and without reinforcement

Table 1: Configurations of the printed samples evaluated

Configuration	Description	Lay-up	No. of Layers	Roofs	Floors	Walls
MF	Markforged specimens	Uni-directional	Unknown	No	No	No
CC	Concentric	Uni-directional	8	Yes	Yes	Yes
QI	Quasi-isotropic	[0/45/90/-45] _s	8	Yes	Yes	Yes
OO	Onyx™	NA	8	Yes	Yes	Yes

A summary of the materials evaluated with the different configurations are shown in Table 1. The number of layers contained in the specimens provided by Marforged are unknown as the company did not disclose these manufacturing details. An image of the cross-section of the fibre orientation as generated by the Eiger software is shown in Figure 3. The white lines in the image represent the Onyx™-only walls.

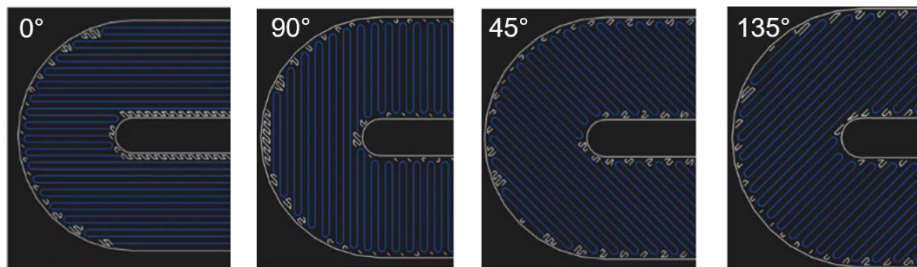


Figure 3: Cross-section of the specimens showing different fibre orientations

2.2 Machining of the Specimens

The AM racetrack specimens were cut to size (following the dashed lines in Figure 2) to create specimens as per ASTM D3039 [6] with dimensions of 254 mm by 12.7 mm. These coupons were used to evaluate the quasi-static tensile properties of the materials. A water-cooled diamond saw with a 2 mm thick blade at 4200 RPM was used for the machining operations. The blade was raised to its highest position and the sample was clamped as close as possible to the cut line, as shown in Figure 4. To cut the specimen, the blade was moved towards the racetrack very slowly until reaching the middle position (label 1, in Figure 4). The blade was then brought back to its initial position and progressed to cut the second half of the specimen (label 2, in Figure 4). This method was effective in preventing

damage, deformation, and delaminations of the material. A representative image of an offcut of a delaminated sample is shown in Figure 5, top. This image was obtained from an off-cut of a “dummy” sample using an Olympus optical microscope at 50X magnification. In this micrograph, the detachment of the bottom-most layer is evident and highlights the importance of developing a machining procedure to avoid damaging the samples while cutting. Figure 5, bottom, shows the image of an offcut for which the outlined procedure was followed, with no delaminations present.

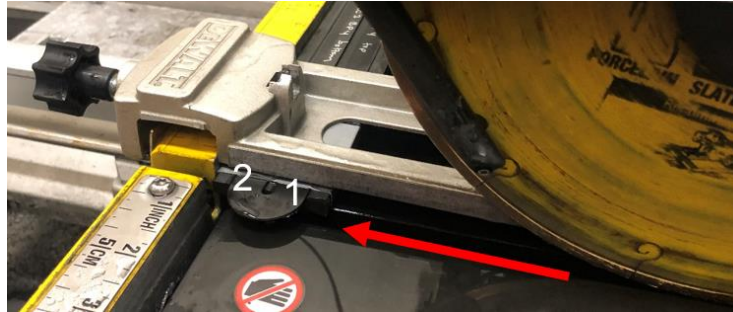


Figure 4: Setup used to machine the racetrack specimens with a water-cooled diamond saw. The arrow indicates the feed direction of the blade

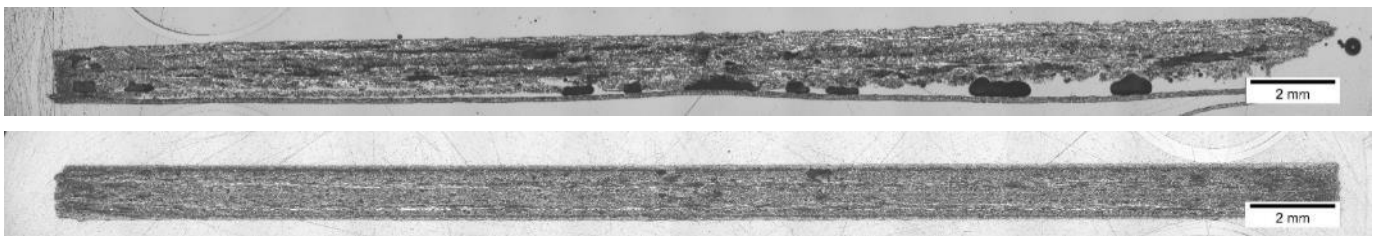


Figure 5: Representative cross-section of a delaminated sample (top) versus a sample which did not suffer damage due to the machining process (bottom)

The resulting specimen to be tested is shown in Figure 6.



Figure 6: Machined sample to be tested as per ASTM D3039

2.3 Mechanical Testing: Quasi-Static Tensile Tests

The test method defined in ASTM D3039 [6] was used to evaluate the quasi-static tensile properties of the material. Ten samples for each configuration were evaluated with the exception of the specimens provided by Markforged (only four specimens were available). The tests were performed at room temperature under displacement control at a rate of 1.3 mm/min in a MTS 810 loadframe. A 50 kN load cell was used to test the MF, CC, and QI specimens, whereas a 10 kN load cell with a piggyback adapter was used to test the OO samples. Surfalloy hydraulic grips with a gripping force of 3.45 MPa were used for the test. Mesh grit was used at the location where the sample contacted the grips. A MTS LX 500 laser extensometer was used to measure strain. The setup used for testing is shown in Figure 7.

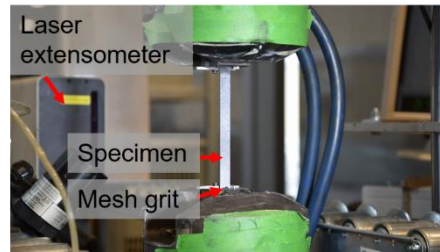


Figure 7: Test setup used to evaluate the AM samples as per ASTM D3039 using a laser extensometer to measure strain

2.4 Mechanical Testing: Fatigue in Tension-Tension

After completing the quasi-static tensile tests, ASTM D3479 [7] was followed to evaluate fatigue performance in tension-tension for the samples with the QI configuration only. This configuration was selected due to design considerations of the final product. A total of twelve specimens were tested up to 25% (one specimen), 50% (seven specimens), 65% (three specimens) and 80% (one specimen) of the ultimate tensile strength (UTS), which was determined from the quasi-static tensile tests. The specimens were machined following the procedure outlined in Section 2.2 to the same dimensions as the specimens tested as per ASTM D3039. A load ratio value of $R=0.1$ was used at a frequency of 5 Hz to test the samples up to 10^6 cycles at room temperature. To evaluate if there was accumulation of damage within the sample due to fatigue, a modulus check was performed before and after each fatigue test (i.e., the modulus check after the test was conducted only if the specimen withstood 10^6 cycles). During the modulus check, the specimen was loaded quasi-statically up to 25% of the UTS. A decreased stiffness was considered to be indicative of microcrack occurrence. An image was captured at the end of each modulus check using Digital Image Correlation (DIC). In addition, a K-type thermocouple was placed on the gauge area on each sample to monitor the thermal history during the fatigue test, as recommended by CMH-17 [8]. In fatigue testing of polymer composites, internal viscoelastic effects can cause an increase in temperature, which can change the test condition and the material properties. Therefore it is recommended to reduce the frequency if a temperature of more than 3 C is measured. The setup is shown in Figure 8.

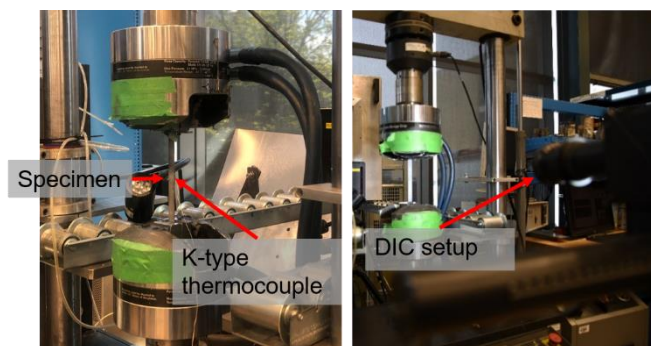


Figure 8: Test setup used to evaluate the AM samples as per ASTM D3479 for fatigue in tension-tension. A K-type thermocouple was placed at the gauge area to monitor viscoelastic effects during the test. DIC was setup to capture an image after each of the modulus checks

2.5 Microscopy

The surfaces of the fractured tensile samples were analyzed using a Carl Zeiss Sartzoom 5 stereomicroscope at a magnification of 5x. Additional evaluation of a failed sample due to fatigue was performed by Scanning Electron Microscopy (SEM) using a JCM-7000 NeoScope™ SEM microscope at 75X, 200X and 500X magnifications.

3 RESULTS AND DISCUSSION

3.1 Mechanical Testing: Quasi-Static Tensile Tests

The tensile strength and modulus of each configuration are shown in Figure 9 and summarized in Table 2. The CC configuration attained the highest strength due to the load being applied in the same direction as the continuous fibres. These values matched closely the values reported in the Markforged datasheet (Table 2). On the other hand, the values of the OO samples are lower than those reported by Markforged and measured following ASTM D638 in their data sheet. The difference in test methodologies may have contributed to these discrepancies. The Onyx™ roofs and floors did not seem to have a significant effect on the mechanical performance, as similar results were obtained between the MF and CC configurations.

Table 2: Summary of the quasi-static tensile test results

Configuration	Datasheet Tensile Strength (MPa)	Average Tensile Strength (MPa)	CV ^c (%)	Average Tensile Modulus (GPa)	CV (%)
MF	760 ^a	647	8.5	57	3.4
CC	-	707	9.5	54	4.0
QI	-	245	7.0	18	2.9
OO	40 ^b	29.2	4.4	0.4	23.0

^a Tested as per ASTM D3039; ^b Tested as per ASTM D638; ^c Coefficient of Variance

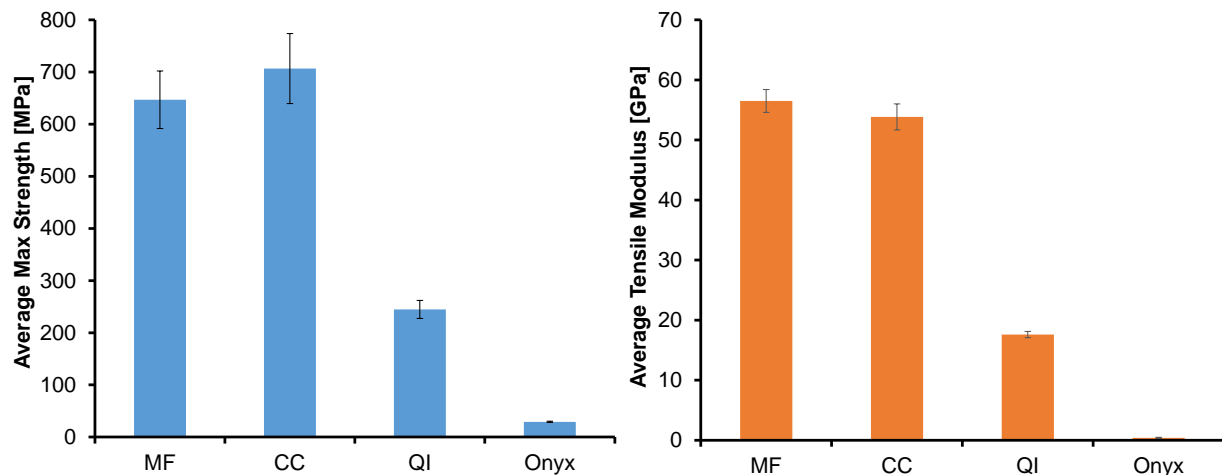


Figure 9: Tensile strength and tensile modulus of printed specimens following ASTM D3039. The error bars were calculated using one standard deviation

The failure modes of the fractured samples were analyzed and classified as per the standard. These are summarized in Table 3. A representative photo of each specimen type is shown in Figure 10. Overall, similar failure modes were observed for the MF and CC samples, which were driven by the orientation of the fibres (i.e., oriented in the loading direction). The QI samples displayed mostly angled failures driven by the presence of the 45° angled plies, whereas the OO configuration displayed brittle failure.

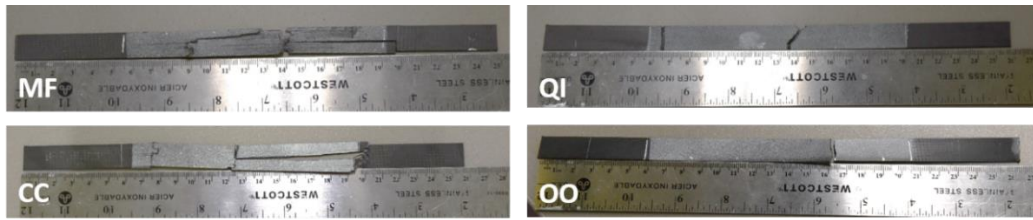


Figure 10: Representative images showing the predominant failure mode of each specimen type

Table 3: Summary of failure modes and their definitions which were observed after the quasi-static tensile tests

Configuration	Description	Failure Mode	Failure Type	Failure Area	Failure Location
MF	Markforged specimens	LAV, LAB	Lateral	At grip	Bottom and various regions of the gauge section
		SGM	Long splitting	In the gauge section	Middle of the gauge section
CC	Concentric	LAV, LAT	Lateral	At the grip	Top and various regions of the gauge section
		SGB, SGM, SGV	Long splitting	In the gauge section	Bottom, middle and various regions of the gauge section
QI	Quasi-isotropic	AGM, AGV, AAV	Angled	In gauge and grip sections	Middle and various regions of the gauge section
		LGT, LAT	Lateral	In gauge and grip sections	Top of the gauge section
OO	Onyx™-only	AGM	Angled	In gauge section	At the middle of the gauge section
		LGM, LGT	Lateral	In gauge section	Top and middle of the gauge section

3.2 Mechanical Testing: Fatigue in Tension-Tension

The average UTS of the QI samples was 245 MPa ± 17.2 MPa. Specimens were tested in fatigue at maximum load levels of 25%, 50%, 65%, and 80% of the UTS. A modulus check was performed before and after each fatigue test (for those specimens that survived), where the specimen was loaded quasi-statically up to 61.3 MPa (i.e., 25% of the UTS). The representative results for one of the samples is shown in Figure 11. The modulus was obtained by measuring the slope. For the sample shown below, the modulus decreased by 0.7 GPa after the fatigue test, from 17.2 GPa to 16.5 GPa. Overall, this reduction in modulus of 4% suggests there was some accumulation of damage in the specimen, however the reduction was not considered to be significant. An image was taken using DIC at the end of each modulus check step, as shown in Figure 11. The images show small regions over the surface with higher local strains. Overall the values of strain were 10% higher for those specimens tested after the sample survived 10⁶ cycles.

During the fatigue test, the specimen temperature remained stable with an increase of approximately 3°C after taking into consideration fluctuations due to the increase in ambient temperature. Typical temperature measurements are shown in Figure 12. The difference between the sample and the ambient temperature were attributed to the error of the measuring devices. This increase in specimen temperature was deemed acceptable and the testing frequency of 5 Hz was maintained for all specimens, as it was not considered to significantly change the testing conditions.

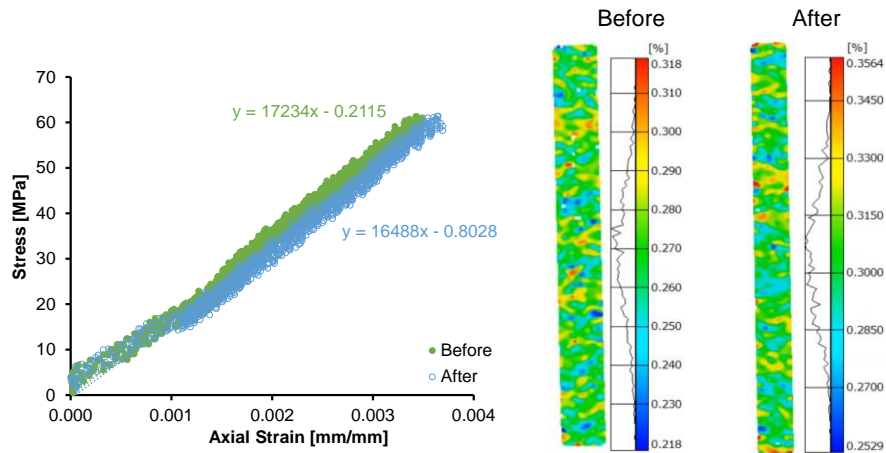


Figure 11: Modulus check results before and after the fatigue test (left) along with the images captured using DIC (right)

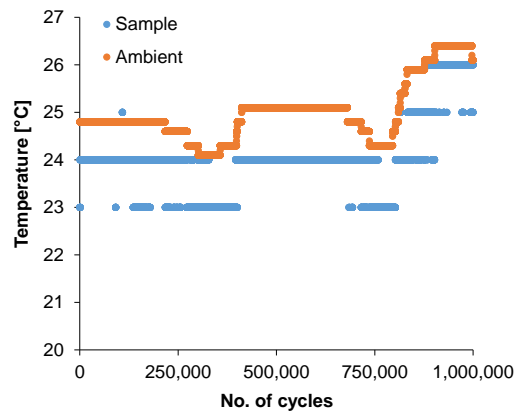


Figure 12: Thermocouple data monitoring the temperature during a fatigue test for a sample loaded up to 25% UTS

Samples tested at 50% or less of the UTS had similar results. Figure 13 shows the maximum stress vs. cycles (N_f) to failure of the specimens. A summary of the fatigue results, including the modulus check are summarized in Table 4. Coupons tested at 65% of the UTS showed significant variability without surviving the full test range. The specimen tested at 80% of the UTS failed after only 10^3 cycles.

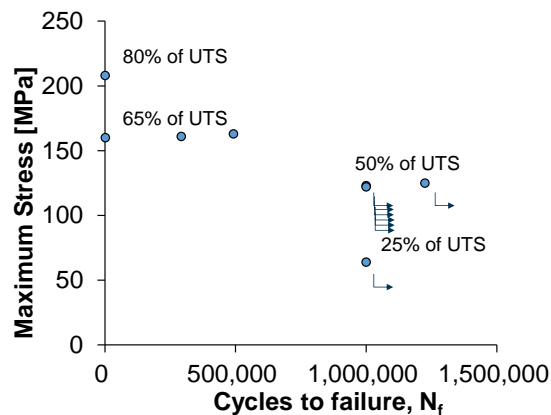


Figure 13 Maximum stress vs. cycles to failure of AM QI specimens

Table 4: Summary of the fatigue test results, including modulus check for AM samples in QI configuration

No. of Test	%UTS	Test Conditions		Modulus Check		Fatigue Test
		Max Load (N)	Min Load (N)	Modulus before test (GPa)	Modulus after test (GPa)	No. of Cycles to Failure
1	25	1130	113	21.4	27.6	>10 ⁶
2	50	2260	226	17.2	16.5	>10 ⁶
3	50	2260	226	16.7	15.4	>10 ⁶
4	50	2260	226	17.5	15.3	>10 ⁶
5	50	2260	226	17.3	16.6	>10 ⁶
6	50	2260	226	16.5	11.5	>10 ⁶
7	50	2260	226	16.1	12.6	>10 ⁶
8	50	2260	226	17.2	16.1	>10 ⁶
9	65	2938	293.8	18.7	N/A	492 010
10	65	2938	293.8	16.3	N/A	291 991
11	65	2938	293.8	16.0	N/A	1463
12	80	3652	365.2	17.3	N/A	954

3.3 Microscopy

The images of the fractured samples from the quasi-static tensile tests are shown in Figure 14. Upon closer observation, the MF and QI samples show delaminations between layers (i.e., towards the top of the figure). In FFF, the layer-to-layer interface is known to be weak, particularly in the z-direction tensile strength. This weakness caused anisotropy of the printed specimens. The weakest direction remains an important determinant in the performance of the final printed part [9].

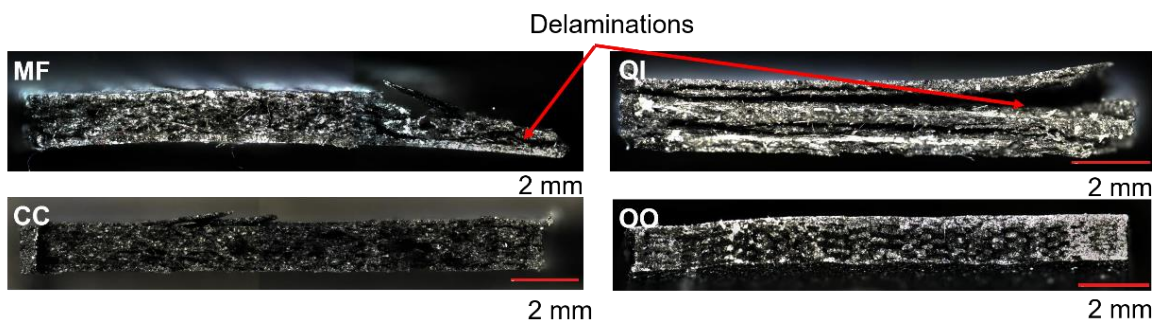


Figure 14: Images of the fractured interfaces of the MF (top left), CC (bottom left), QI (top right) and OO (bottom right) samples obtained with the stereomicroscope at 5X magnification

The QI sample at 80% of UTS in fatigue was imaged using SEM. Figure 15, left, shows areas with delaminations or voids present in the sample. When looking closer at these regions, it can be observed that these regions seem to show a lack of complete welding between layers (Figure 15, centre, and right). It is possible that these regions acted as stress concentrations, which led to the rapid failure when tested at this high loading condition.

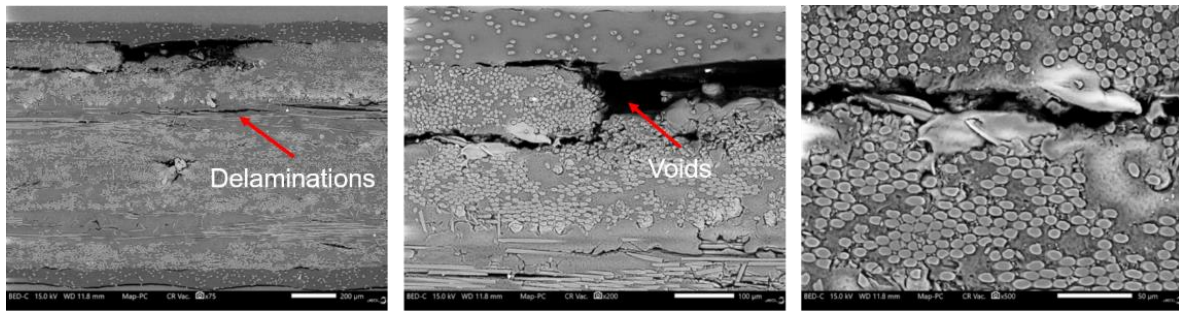


Figure 15: SEM image at 75X (left), 200X (centre) and 500X (right) of the QI sample tested in fatigue (80% of the UTS)

4 CONCLUSION

In this work, the FFF concentric specimens displayed the highest performance in the quasi-static tensile tests due to the alignment of all the reinforcement (i.e., the fibres) in the loading direction. Their performance was similar to that observed in the MF specimens supplied by Markforged. Of the quasi-isotropic configuration samples tested in R=0.1 tension-tension fatigue at 25%, 50%, 65% and 80% of the quasi-static UTS, only the samples tested at 25% and 50% survived the full duration of 10^6 cycles. The samples tested at 65% displayed significant variability in the number of cycles to failure. Micrographs of the fracture surfaces in the quasi-static tensile specimens showed voids and regions of delaminations, which can be attributed to defects and regions of weakness created during the printing process. These may have induced stress concentrations, which contributed to failure during these tests. Overall, these tests provided a deeper understanding of the tensile (quasi-static and fatigue) properties of parts made using the FFF process. Depending on the final goal of a specific part, additional tests may be needed in order to have a full picture with statistical representation of the mechanical properties of the structure.

5 ACKNOWLEDGEMENTS

The authors of this paper would like to give special thanks to Hugo Laurin, Richard Desnoyers and Maxime Guérin for their help and contributions in preparing the samples, and for their help to test the specimens.

6 REFERENCES

- [1] F. Ning, W. Cong, et al., “Additive manufacturing of carbon fiber-reinforced plastic composites using fused deposition modeling: Effects of process parameters on tensile properties”. *Journal of Composite Materials*. Vol. 5 (4), pp 451-462. 2017
- [2] S. Kumar, R. Singh, et al. “Fused filament fabrication: A comprehensive review”. *Journal of Thermoplastic Composite Materials*. pp 1-21. 2020
- [3] A. Maguire, N. Pottackal, et al. “Additive manufacturing of polymer-based structures by extrusion technologies”. *Oxford Open Materials Science*. Vol 1 (1), 2021
- [4] Markforged. <https://markforged.com/fr/3d-printers/x7>, 2022, (Accessed on February 28th, 2022).
- [5] Markforged. “Material Datasheet Composites”. Rev 5.2. Watertown, MA. 20-Jan-2022
- [6] ASTM D3039-08. “Standard Test Method for Tensile Properties of Polymer Matrix Composite Materials”. *ASTM International*. West Conshohocken, PA, USA.
- [7] ASTM D3479-19. “Standard Test Method for Tension-Tension Fatigue of Polymer Matrix Composites
- [8] Composite Materials Handbook 17G, Volume 1 “Polymer Matrix Composites: Guidelines for Characterization of Structural Materials”, Section 2.5.14.
- [9] K. Rodzen, E. Harkin-Jones, et al. “Improvement of the layer-layer adhesion in FFF 2D printed PEEK/carbon fibre composites”. *Composites Part A: Applied Science and Manufacturing*. Vol. 149 (106532), 2021